Science Advances
AAAS

Supplementary Materials for

Single-nucleosome imaging reveals steady-state motion of interphase chromatin in living human cells

Shiori Iida *et al.*

Corresponding author: Kazuhiro Maeshima, kmaeshim@nig.ac.jp

Sci. Adv. **8**, eabn5626 (2022)
DOI: 10.1126/sciadv.abn5626

The PDF file includes:

Other Supplementary Material for this manuscript includes the following:

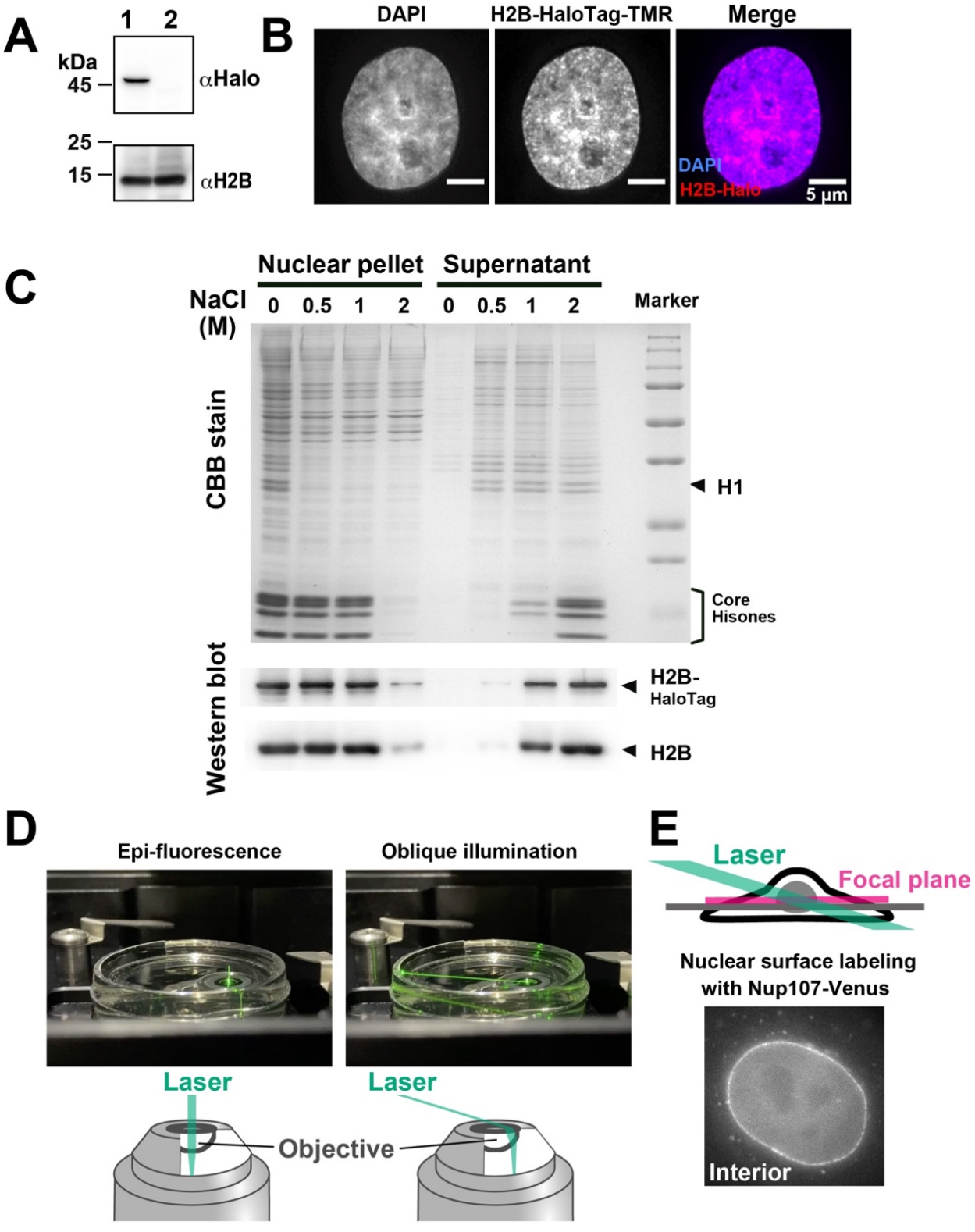
A
1 2
kDa
45
αHalo
25
15
αH2B
B
DAPI
H2B-HaloTag-TMR
Merge
DAPI
H2B-Halo
5 μm
C
Nuclear pellet
Supernatant
NaCl (M)
0 0.5 1 2 0 0.5 1 2
Marker
CBB stain
H1
Core Hisones
Western blot
H2B-HaloTag
H2B
D
Epi-fluorescence
Oblique illumination
Laser
Laser
Objective
E
Laser
Focal plane
Nuclear surface labeling with Nup107-Venus
Interior

Figure S1

Fig. S1. Expression level and behavior of H2B-Halo in HeLa cells and oblique illumination microscopy

(A) Expression of H2B-Halo in HeLa cells was confirmed by Western blotting with α-Halo antibody (lane 1). In lane 2, parental HeLa cells show no H2B-Halo signals. **(B)** HeLa cells expressing H2B-Halo fluorescently labeled with excess amounts of TMR-HaloTag ligand (center). The left panel is DNA stained with DAPI. The merged image (DNA, blue; H2B-Halo, red) is shown at right. Note that the TMR labeling pattern is very similar to the DNA staining one. **(C)** Stepwise salt washing of nuclei isolated from the established cells expressing H2B-Halo. The nuclei isolated from HeLa cells expressing H2B-Halo were washed with the indicated buffers including various concentrations of NaCl. The resultant nuclear pellets (left) and supernatants (right) were analyzed by SDS-PAGE, and subsequently stained with Coomassie brilliant blue staining (top) or immunoblotted for H2B (bottom). Positions of core histones and linker histone H1 are indicated in Coomassie brilliant blue stain. Biochemical behaviors of H2B-Halo and endogenous H2B were checked by Western blot with the anti-H2B antibody. Note that H2B and H2B-Halo started to dissociate from chromatin with 1 M NaCl and were detected in the supernatant fraction, suggesting that H2B-Halo was incorporated into nucleosome structures similar to that of endogenous H2B. **(D)** Images of epi-fluorescence (left) and oblique illumination (right) in the glass-based dishes filled with medium. **(E)** Oblique illumination for the nuclear interior of HeLa cells expressing a nuclear pore component NUP107-Venus, which labeled the nuclear envelope (*47*). The nuclear rim was clearly seen by the laser beam (green), indicating that a focal plane (pink) around the nuclear interior was illuminated with the microscopy setting used.

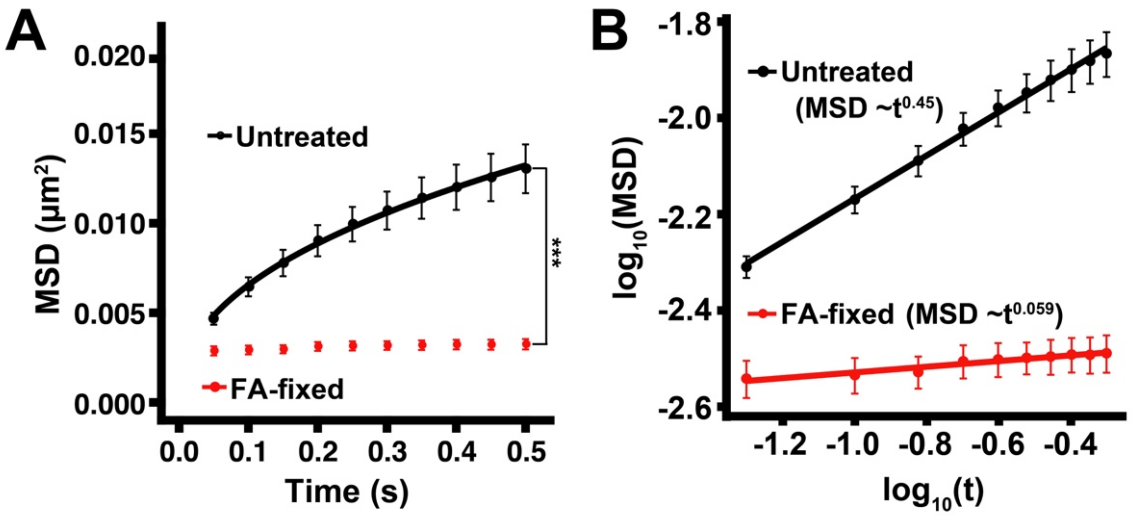

Figure S2

Fig. S2. MSD plots of the nucleosome motion in a tracking time range from 0.05 to 0.5 s. **(A)** MSD plots (± SD among cells) of the nucleosome motion in untreated control (black) and FA-fixed (red) HeLa cells from 0.05 to 0.5 s. For each sample, n = 10–15 cells. ***$P < 0.0001$ ($P = 6.2 \times 10^{-7}$) by Kolmogorov–Smirnov test. **(B)** Log–log plot of MSD from the plot of (A). The plots were fitted linearly; $MSD = 0.018t^{0.45}$ in living untreated control cells and $MSD = 0.0034t^{0.059}$ in FA-fixed cells.

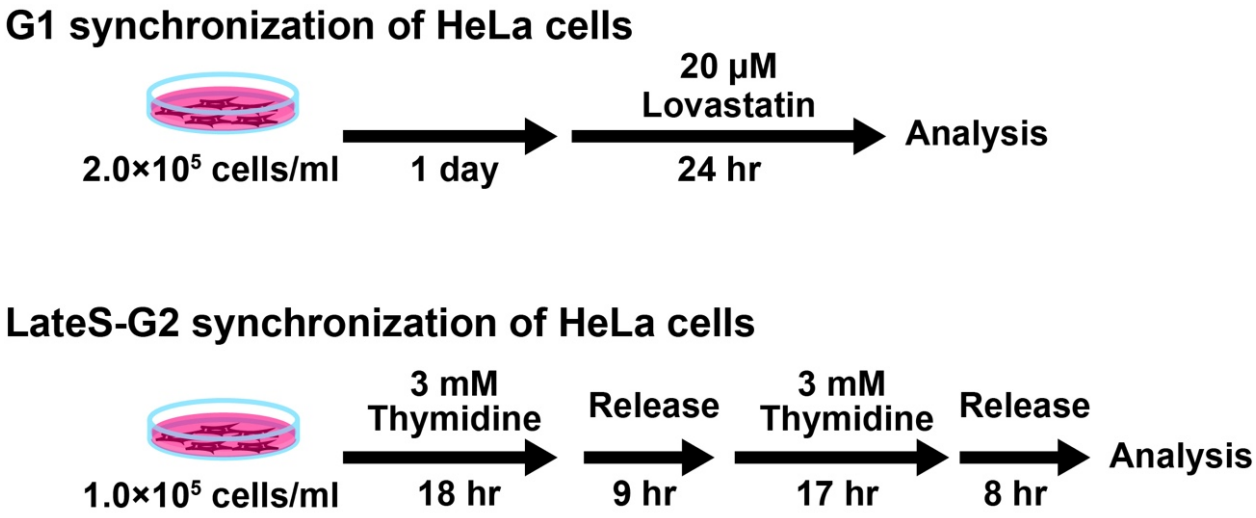

Figure S3

Fig. S3. Scheme for synchronization of HeLa cells in G1 and LateS-G2 phases.

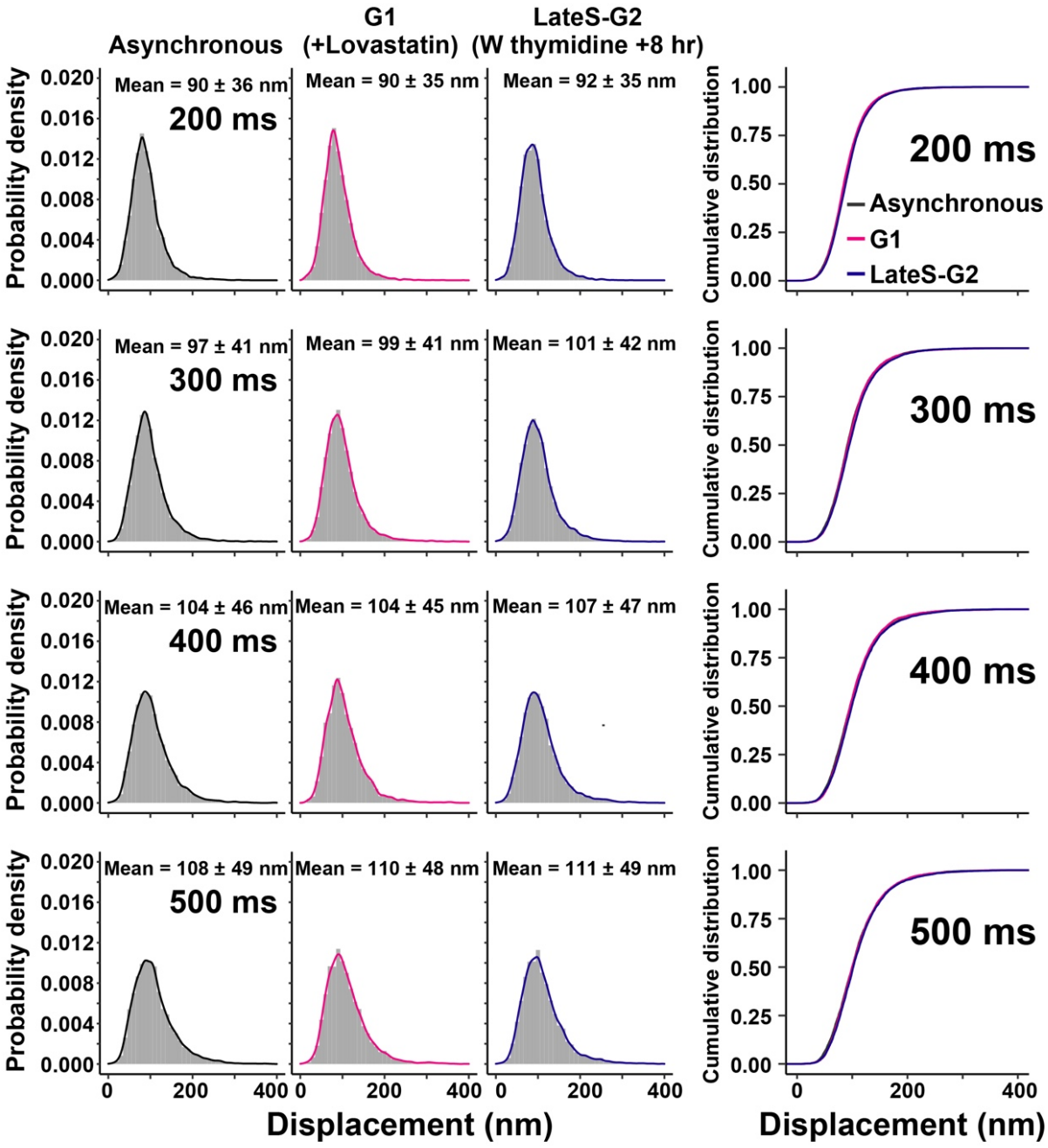
Asynchronous
G1 (+Lovastatin)
LateS-G2 (W thymidine +8 hr)
Probability density
Cumulative distribution
Mean = 90 ± 36 nm
Mean = 90 ± 35 nm
Mean = 92 ± 35 nm
200 ms
Mean = 97 ± 41 nm
Mean = 99 ± 41 nm
Mean = 101 ± 42 nm
300 ms
Mean = 104 ± 46 nm
Mean = 104 ± 45 nm
Mean = 107 ± 47 nm
400 ms
Mean = 108 ± 49 nm
Mean = 110 ± 48 nm
Mean = 111 ± 49 nm
500 ms
Asynchronous
G1
LateS-G2
Displacement (nm)

Figure S4

Fig. S4. Displacement distribution histograms of single nucleosomes in Asynchronous, G1 and LateS-G2 cells.
Left, Histograms of single nucleosomes (n = 15 cells) for 200 ms, 300 ms, 400 ms and 500 ms of Asynchronous, G1 (+Lovastatin) and LateS-G2 (W thymidine block + 8 hr) cells. Asynchronous data were reproduced from Fig. 1E. Mean ± SD of displacement is indicated at the top. Note that the shape of the displacement distribution is similar for Asynchronous, G1 and LateS-G2. Right, cumulative distribution plots of the displacement.

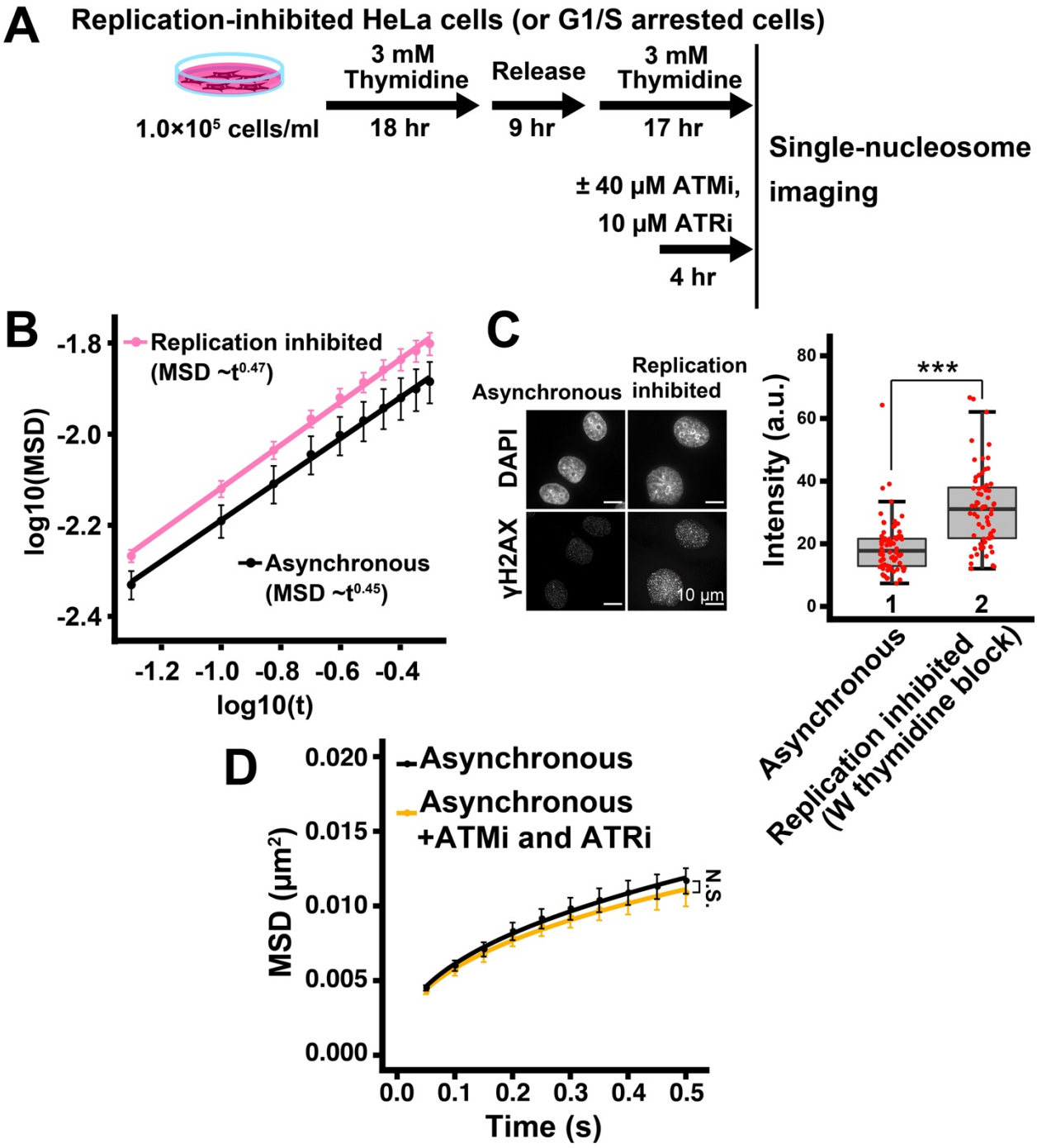
A
Replication-inhibited HeLa cells (or G1/S arrested cells)
1.0×10⁵ cells/ml
3 mM Thymidine
18 hr
Release
9 hr
3 mM Thymidine
17 hr
± 40 μM ATMi, 10 μM ATRi
4 hr
Single-nucleosome imaging
B
Replication inhibited (MSD ~t^0.47)
Asynchronous (MSD ~t^0.45)
log10(MSD)
log10(t)
C
Asynchronous
Replication inhibited
DAPI
γH2AX
10 μm
Intensity (a.u.)
***
Asynchronous
Replication inhibited (W thymidine block)
D
Asynchronous
Asynchronous +ATMi and ATRi
MSD (μm²)
Time (s)
N.S.

Figure S5

Fig. S5. DNA replication inhibition in HeLa cells, log-log plot of their nucleosome MSD data, verification of their γH2AX signals, and effect of ATMi and ATRi on local chromatin motion in asynchronous cells.

(A) Scheme of the preparation for DNA replication-inhibited (G1/S arrested) HeLa cells. **(B)** Log-log plot of the MSD data from Fig. 5E. Asynchronous data was reproduced from Fig. S2B. The plots were fitted linearly; MSD = $0.018t^{0.45}$ in Asynchronous cells and MSD = $0.023t^{0.47}$ in Replication inhibited cells. **(C)** Left, verification of the γH2AX signals by immunostaining. Right, box plots of γH2AX signal intensity. Median values: lanes 1 (17.8, n = 75 cells); 2 (31.4, n = 66 cells). ***, $P < 0.0001$ ($P = 8.1 \times 10^{-11}$) by Wilcoxon rank sum test. **(D)** MSD plots (± SD among cells) of nucleosome motions in Asynchronous (black) and Asynchronous + ATMi and ATRi (red) HeLa cells from 0.05 to 0.5 s. Nucleosome trajectories used per cell: 2200–2270; n = 15 cells per sample. Not significant (N.S.; $P = 0.18$) by Kolmogorov–Smirnov test.

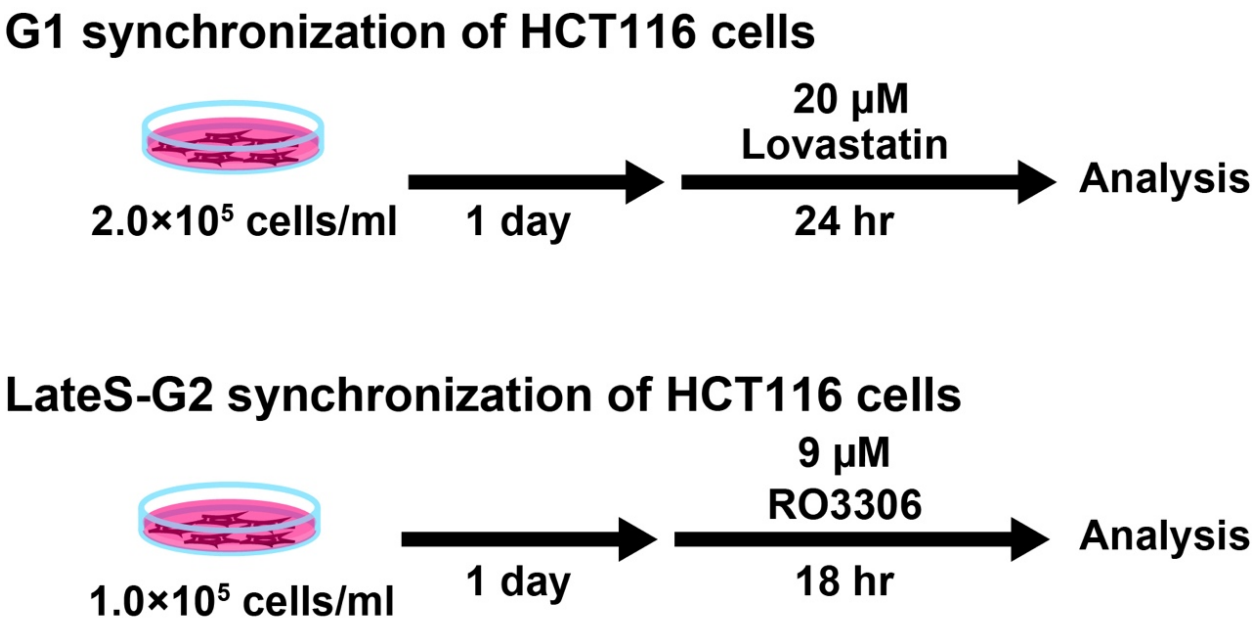

Figure S6

Fig. S6. Schematic for synchronization of HCT116 cells in G1 or LateS-G2 phase.

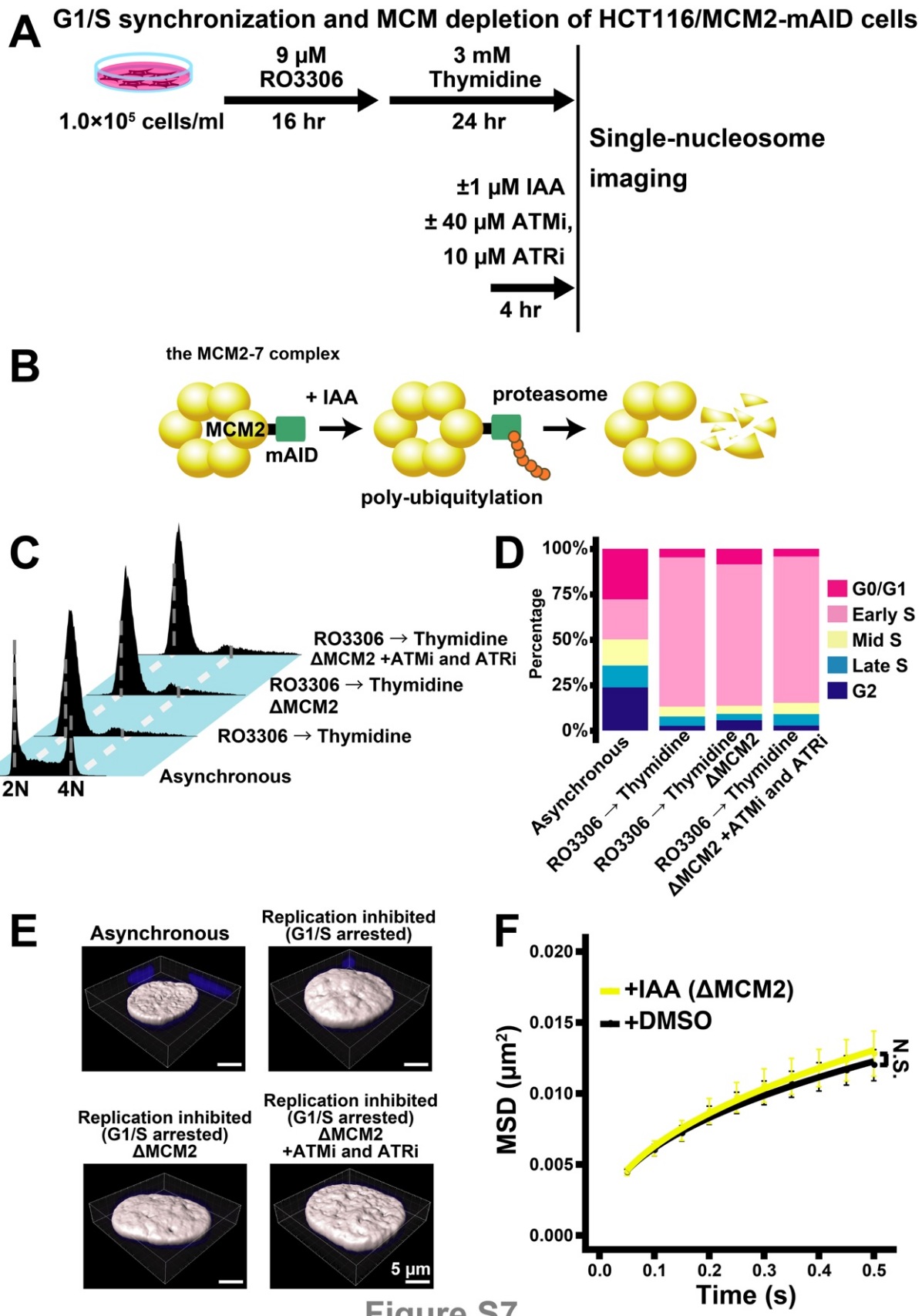
A
G1/S synchronization and MCM depletion of HCT116/MCM2-mAID cells
1.0×10⁵ cells/ml
9 μM RO3306
16 hr
3 mM Thymidine
24 hr
±1 μM IAA
± 40 μM ATMi,
10 μM ATRi
4 hr
Single-nucleosome imaging
B
the MCM2-7 complex
MCM2
mAID
+ IAA
proteasome
poly-ubiquitylation
C
RO3306 → Thymidine ΔMCM2 +ATMi and ATRi
RO3306 → Thymidine ΔMCM2
RO3306 → Thymidine
Asynchronous
2N
4N
D
Percentage
100%
75%
50%
25%
0%
G0/G1
Early S
Mid S
Late S
G2
Asynchronous
RO3306 → Thymidine
RO3306 → Thymidine ΔMCM2
RO3306 → Thymidine ΔMCM2 +ATMi and ATRi
E
Asynchronous
Replication inhibited (G1/S arrested)
Replication inhibited (G1/S arrested) ΔMCM2
Replication inhibited (G1/S arrested) ΔMCM2 +ATMi and ATRi
5 μm
F
+IAA (ΔMCM2)
+DMSO
N.S.
MSD (μm²)
0.020
0.015
0.010
0.005
0.000
0.0
0.1
0.2
0.3
0.4
0.5
Time (s)

Figure S7

Fig. S7. DNA replication inhibition and MCM2 depletion in HCT116 cells, validation and nuclear reconstruction of replication-inhibited HCT116 cells, and effect of MCM2 depletion on local chromatin motion in asynchronous cells.

(A) Scheme of preparation for DNA replication-inhibited (G1/S arrested) HCT116 cells. **(B)** In HCT-116/MCM2-mAID cells, both MCM2 alleles are tagged with auxin inducible degrons and the AtAFB2 gene is integrated at the AAVS1 locus. Auxin treatment (IAA) leads to proteasomal degradation of MCM2. **(C)** Cellular DNA contents in indicated HCT116 cell populations measured by flow cytometry. Note that neither MCM2 degradation nor treatment of the inhibitors affects the cell cycle profile. Each histogram represents more than 25,000 cells. **(D)** Quantification from Fig. S7C data. 82% of cells in "RO3306 → thymidine" are in early S phase. 78% of cells in "RO3306 → thymidine, ΔMCM2" are in early S phase. 81% of cells in "RO3306 → Thymidine, ΔMCM2 + ATMi and ATRi" are in early S phase. **(E)** Reconstructed 3D images of HCT116 nuclei with indicated conditions. **(F)** MSD plots (± SD among cells) of nucleosome motions in DMSO treated asynchronous (black) and IAA treated (MCM2 depleted) asynchronous cells (yellow) from 0.05 to 0.5 s. Nucleosome trajectories used per cell: 2110-2170; n = 15 cells per sample. Not significant (N.S.; P = 0.68) by Kolmogorov–Smirnov test.

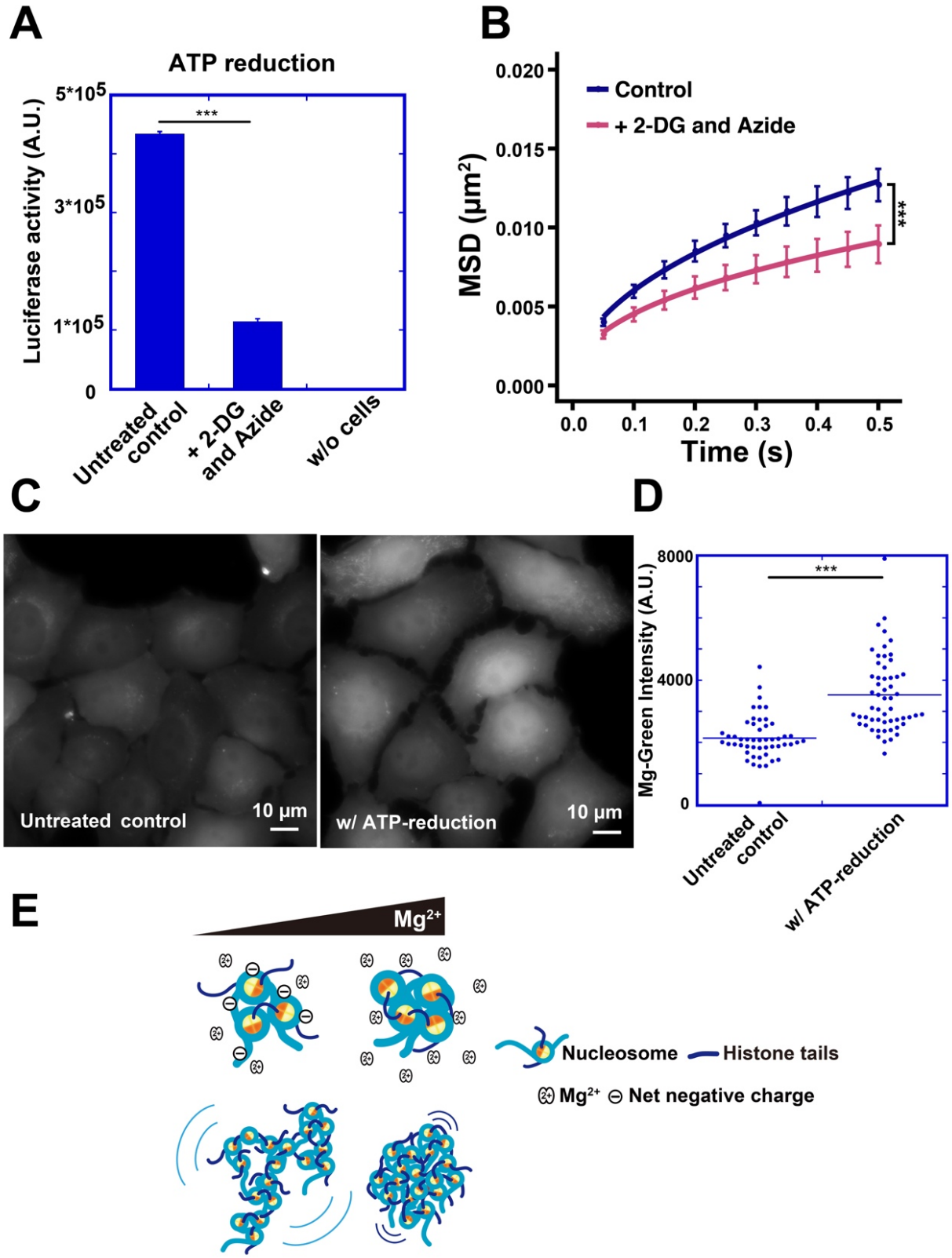
A
ATP reduction
Luciferase activity (A.U.)
5*10^5
3*10^5
1*10^5
0
***
Untreated control
+ 2-DG and Azide
w/o cells
B
MSD (μm²)
0.020
0.015
0.010
0.005
0.000
Control
+ 2-DG and Azide
***
0.0
0.1
0.2
0.3
0.4
0.5
Time (s)
C
Untreated control
10 μm
w/ ATP-reduction
10 μm
D
Mg-Green Intensity (A.U.)
8000
4000
0
***
Untreated control
w/ ATP-reduction
E
Mg2+
Nucleosome
Histone tails
Mg2+ Net negative charge

Figure S8

Fig. S8. Decrease in local chromatin motion and increase in free Mg^{2+} level in ATP-reduced cells.

(A) Luciferase-based adenosine triphosphate (ATP) measurements for HeLa cells: untreated cells (left), cells treated with 2-DG and sodium azide (center) and without cells (right). Bars represent the SD (n = 9). ***p < 0.0001 ($p = 1.2 \times 10^{-26}$) by Student's t test. **(B)** MSD plots (± SD among cells) of nucleosome motions in MQ treated control cells (blue) and cells treated with 2-DG and sodium azide (pink) from 0.05 to 0.5 s. Nucleosome trajectories used per cell: 769-902; n = 12-14 cells per sample. ***P < 0.0001 ($P = 2.7 \times 10^{-6}$) by the Kolmogorov–Smirnov test. **(C)** Quantification of intranuclear free Mg^{2+} levels by Mg-Green fluorescent signal. **(D)** Quantitative data of Mg-Green signal intensity. For each sample, n = 51-56 cells. ***, P < 0.0001 ($P = 3.2 \times 10^{-11}$) by the Wilcoxon rank sum test. **(E)** Schematic of how increasing Mg^{2+} concentration leads to chromatin condensation.

Movie S1.

Movie data (50 ms/frame) of single nucleosomes labeled with TMR in a living HeLa cell recorded by sCMOS ORCA-Fusion BT camera (Hamamatsu Photonics). Note that clear and well-separated dots are visualized with a single-step photobleaching profile after background subtraction (see right, Fig. 1C), suggesting that each dot represents a single H2B-Halo-TMR molecule in a single nucleosome.

Movie S2.

Brownian dynamics simulations of open ($d_f = 1.7$) and compact ($d_f = 2.5$) fractal polymers (Fig. 2D). The 1000-monomers are colored by the RedWhiteBlue gradation. Here, we carried out 250 steps of numerical integration to visualize dynamics.

Movie S3.

Reconstructed 3D movie of a typical HeLa cell nucleus from z-stack images.

Movie S4.

Movie data (50 ms/frame) of single nucleosomes labeled with TMR in a G1-synchronized HeLa cell recorded by sCMOS ORCA-Fusion BT camera (Figs. 3D and 4A). Note that its motions are similar to those of the G2-synchronized cell (see Movie S5).

Movie S5.

Movie data (50 ms/frame) of single nucleosomes labeled with TMR in a G2-synchronized HeLa cell recorded by sCMOS ORCA-Fusion BT camera (Figs. 3D and 4A). Note that the nuclear size in the G2 cell is larger than that in the G1 cell (Movie S4) but the nucleosome motions are similar between the G1 and G2 cells.

Movie S6.

Movie data (50 ms/frame) of a single TetR-4xmCh focus in a G1-synchronized HT-1080 cell recorded by sCMOS ORCA-Flash4.0 camera (Hamamatsu Photonics) (Figs. 9B and 9G). Left: TetR-4xmCh movie of a living G1-phase HT-1080 nucleus after background subtraction. Right, tracking movie by Trackmate plugin on the focus in the left movie. The backward tracts observed over time (30 time points) are indicated by the pink line. The same trajectory is shown in Fig. 9C, left.

Movie S7.

Movie data (50 ms/frame) of double TetR-4xmCh foci in a LateS-G2 synchronized HT-1080 cell recorded by sCMOS ORCA-Flash4.0 camera (Figs. 9B and 9G). Left, TetR-4xmCh movie of a living LateS-G2 phase HT-1080 nucleus after background subtraction. Right, tracking movie by Trackmate plugin on the foci in the left movie. The backward tracts observed over time (30 time

points) are indicated by the pink and light blue lines. The same trajectories are shown in Fig. 9C, right.